Engineering Structures 32 (2010) 195–206

Contents lists available at ScienceDirect

Engineering Structures

journal homepage: www.elsevier.com/locate/engstruct

Lateral pressure over formwork on large dimension concrete blocks

I. Puente *, A. Santilli, A. Lopez

Department of Mechanical Engineering, Institute of Civil Engineering, Tecnun (University of Navarra), Paseo Manuel de Lardizábal 13, 20018 San Sebastian, Spain

ARTICLE INFO

Article history:
Received 27 March 2009
Received in revised form
10 June 2009
Accepted 1 September 2009
Available online 23 September 2009

Keywords:
Concrete
Formwork
Lateral pressure
Finite element
Safety factor

ABSTRACT

The design of vertical formwork is dependent on the lateral pressure predicted to act on the form face. Experimental research into the construction of blocks on a gravity dam was carried out with the objective of verifying and comparing the adequacy of different theories. Pressure was measured indirectly as the load on the trusses of formwork support, which allows verification of the adequacy of the integral of the pressure envelopes, proposed by different authors, using a finite element model in ABAQUS.

An analysis of the relationship between safety and exactitude was carried out with the objective of determining which method apply to formwork design depending on: safety factors, work monitoring, degree of planning and knowledge about the filling process.

It was concluded by recommending the application of different theories based on these parameter values.

1. Introduction

Peurifoy and Oberlender [1], define formwork as a temporary construction designed to mold fresh concrete to the desired size and shape.

Formwork must be sized to support all the weight produced by fresh concrete construction besides the live load itself: materials, equipment and personnel.

The lateral pressure of fresh concrete is a topic of interest to engineers and builders since an overestimation of this value results in an increase of formwork costs which Hurd [2], showed can be up to 60% of the cost of a concrete structure, a fact that is reaffirmed by Kopczynski [3].

On the other hand, an underestimation of the pressure generates pieces made of poor quality or, in a worst case scenario, the failure of the structure.

Hurd [2] states that the objectives in the design process of forms and support elements should be: safety, quality and cost, which makes knowing the lateral pressure of fresh concrete a necessity.

The importance of the subject has being reflected in many technical papers. The most common process of casting a wall or a column consists of placing concrete in lifts, which are subsequently vibrated. The vibrators are submerged into the concrete a length equal to the height of the lift to guarantee the correct consolidation.

Gardner and Quereshi [4], argue that the vibration is performed to fluidize the concrete, destroying its shear strength and friction with the form wall. Once the concrete is completely fluidized it behaves as a fluid so that the lateral pressure is equal to the hydrostatic pressure produced by a fluid with the same density as concrete.

Gardner [5] states that not all the concrete mass is fluidized since deeper layers are not affected by the vibration and so develop shear strength, which allows them to support vertical loads, develop friction between the concrete and the wall, and therefore generate less lateral pressure.

As a conclusion, lateral pressure reaches a maximum at some elevation above the base of the form and then decreases. This process occurs as chemical bonds are established at the lower layers, developing shear strength and friction with the form wall. Gardner and Poon [6] argue that this process is controlled essentially by time and temperature.

Throughout the years two main ways of solving the problem have been developed: formulate an empirical equation from data obtained in laboratories and/or real construction, or develop a conceptual model of the problem using the mechanical and rheological properties of fresh concrete.

2. Lateral pressure of fresh concrete

2.1. Theoretical models

Theoretical models are based on mathematical theories which try to explain the lateral pressure of fresh concrete on formwork; some of them use the relationship for granular materials, given in Eq. (1).

$$P = \lambda_C \gamma H \tag{1}$$

* Corresponding author. Tel.: +34 943219877; fax: +34 943311442.
E-mail address: ipuente@tecnun.es (I. Puente).

0141-0296/$ – see front matter © 2009 Elsevier Ltd. All rights reserved.
doi:10.1016/j.engstruct.2009.09.006

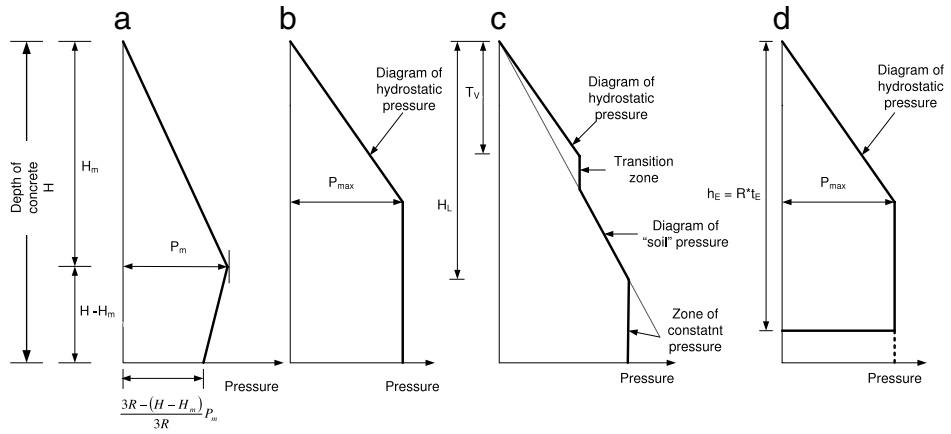

Fig. 1. Different experimental diagrams of pressure envelopes.

where:

- λ_C is the relationship between vertical and horizontal pressure.
- γ is the concrete specific weight.
- H is the concrete depth.

The main problem with these theories is that "λ_C" was not a constant, ranging from one, when concrete acts as a fluid, down to zero, when concrete can self-sustain.

Examples of these theories are developed by: Schödjt [7] and Levitsky [8]; the first one uses concepts of soil mechanics ignoring the cohesion of concrete, while the second uses viscoelastic theory.

The large number of factors related with concrete characteristics, formwork and placing method, which affect the lateral pressure in addition to the friction against the wall and its deformation, generate very complex models which are not used in practice, for formwork design.

2.2. Experimental model

Empirical methods are currently used to predict the pressure and some problems arise when these methods are extrapolated outside the range where experimental data exist.

The ACI Committee 347 [9] and CIRIA Report 108 [10] divided the experimental models into those applied to walls and bases and those used in columns. A wall or a base, are defined as sections where either the width or the breadth exceeds 2 m, while for a column both magnitudes are less than 2 m.

Ritchie [11] and Gardner and Quereshi [4] studied the problem in columns. Johnston et al. [12], Dunston et al. [13], and Arslan et al. [14] studied walls and bases with widths smaller than 1.5 m.

The present study appears as a necessity after having checked the lack of experimental data for concrete pieces with both cross section dimensions greater than 2 m.

Hurd [15], states that the pressure at any given point within the form varies over time; the designer usually does not need to know the variation in detail. The significant magnitude is the maximum pressure envelope that can be applied on the form. Experimental models try to find this pressure envelope depending on the minimum parameters that can be used in the design process. Experimental distribution of wall and base pressures, are presented below:

The most traditional and conservative approach was to consider that fresh concrete has the characteristics of a fluid. In this way, a hydrostatic pressure distribution on the form walls should be considered.

Rodin [16] in 1953 collected and reviewed the published experimental data up to his time, and tried to explain the lateral pressure of fresh concrete against formwork. He concluded that when external vibration is used, the formwork should be designed to support the full hydrostatic pressure of a liquid with the same density as concrete. For internal vibration, he proposed the lateral pressure envelope given in Fig. 1a, where $P_{\max}$ and H_m are expressed in Eqs. (2) and (3), respectively. These equations are valid for a 1:2:4 concrete, with 150 mm slump at a temperature of 21 °C and the concrete density is assumed to be 2400 kg/m^3.

$$H_m = 1.63R^{1/3} \tag{2}$$

$$P_{\max} = 23.4H_m \tag{3}$$

where:

- H_m is the head at which the maximum lateral pressure occurs (m).
- $P_{\max}$ is the maximum lateral pressure against formwork (kPa).
- R is the rate of placement (m/h).

As the equations are developed for a given mix, temperature, density and slump, the author proposes correction curves where the parameters are different.

Adam et al. [17] in 1965 conducted laboratory tests performed on a formwork 3 m high, 2.5 m wide, and with thicknesses ranging from 8 to 30 cm. Their objective was to establish the effect on the lateral pressure of aggregate size, rate of placement, cement type, slump and vibration. They concluded that the most significant variables are: rate of placement, type of cement and aggregate size.

These authors suggested a pressure distribution according to Fig. 1b where the value of $P_{\max}$ is expressed in Eq. (4). This value can never be greater than 23.54H, which is equivalent to the hydrostatic pressure produced by a liquid with a 2400 kg/m^3 density.

When $R < 2$ m/h

$$P_{\max} = 19.62 + 12.26R \quad \text{When } T \leq 5\ ^\circ\text{C} \tag{4a}$$

$$P_{\max} = 19.62 + 9.81R \quad \text{When } T = 15\ ^\circ\text{C} \tag{4b}$$

$$P_{\max} = 19.62 + 8.34R \quad \text{When } T \geq 25\ ^\circ\text{C} \tag{4c}$$

When R > 2 m/h

$$P_{\max} = 40.22 + 1.96R \quad \text{When } T \leq 5\ ^\circ\text{C} \tag{4d}$$

$$P_{\max} = 35.32 + 1.96R \quad \text{When } T = 15\ ^\circ\text{C} \tag{4e}$$

$$P_{\max} = 32.37 + 1.96R \quad \text{When } T \geq 25\ ^\circ\text{C} \tag{4f}$$

where:

- $P_{\max}$ is the maximum lateral pressure against the formwork (kPa)
- R is the rate of placement (m/h)

- H is the concrete depth. (m)
- T is the concrete temperature (°C).

Gardner [18] in 1982, after performing several experimental works, proposed a pressure envelope according to Fig. 1b where the value of P_{max} is given by Eq. (5). The maximum pressure can never be greater than the hydrostatic pressure produced by a fluid with the concrete density. He concluded that the maximum lateral pressure was dependent on the depth of vibration, rate of placement, concrete temperature, slump and percentage of fly ash or slag present in the mix.

$$P_{max} = 24h_i + \frac{3000HP}{d} + \frac{d}{40} + \frac{400R^{1/2}}{18+T} * \left(\frac{100}{100-\%F}\right) + \frac{\alpha - 75}{10} \quad (5)$$

where

- P_{max} is the maximum lateral pressure against formwork (kPa)
- d is the minimum form dimension (mm)
- h_i is the vibration length immersion (m)
- HP is the vibrator's power (HP)
- R is the rate of placement (m/h)
- T is the concrete temperature (°C)
- %F is the percentage of fly ash or slag
- α is the concrete slump (mm).

Gardner [5] in 1985 states that for formwork design the power of the vibrator can be assumed as 3/4 HP per 30.5 cm of smaller form section, to simplify the equation.

The Canadian Standard CSA S269.3 [19] recommended the application of this simplification, when all the parameters presented in Eq. (5) are known in advance.

Palanca [20] in 1982, based on experimental data by CERA Report N° 1 [21] and Gardner [22] proposed a law of pressure distribution with four different zones as shown in Fig. 1c. The first zone, with hydrostatic pressure up to a variable height (T_V), depends on the vibration methods and the depth of each lift. He recommends assuming T_V as the height of the last lift with a maximum of 1.0 m.

Subsequently, there is a transition zone where the pressure is constant until the granular zone. In this zone hydrostatic pressure is affected by a coefficient of active pressure (K_a), which relates vertical and horizontal pressure. This coefficient depends on the internal friction between particles and the inclination of the form wall and is given in Eq. (6).

$$K_a = \frac{\sin^2\left(\frac{\pi}{4} - \frac{\varphi-\varepsilon}{2}\right)}{\cos^2\left(\frac{\pi}{4} - \frac{\varphi+\varepsilon}{2}\right)} \quad (6)$$

where:

- φ is the concrete angle of internal friction. (Palanca [20], based on experimental data by CERA Report N° 1 [21] considers the value given by Eq. (7))
- ε is the inclination of the form wall, from the vertical

$$tg\varphi = \frac{260 - \alpha}{1400} \quad (7)$$

where:

- φ is the concrete angle of internal friction
- α: is the concrete slump (mm)

This distribution is maintained to a depth of pressure limits (H_L) as shown in Fig. 1c, or until the end of the formwork, being determined by two aspects: concrete hardening or formwork thickness. The low rate of placement or reduced thickness leads to the fourth zone of constant pressure until the entire form is covered.

In the case study because of the cross section, the determining factor of the fourth zone is the concrete hardening, where the depth H_L is given in Eq. (8).

$$H_L = T_V + Rt_0 \quad (8)$$

where:

- H_L is the transition depth between the third and fourth zone (m)
- T_V is the transition depth between the first and second zone (m)
- R is the rate of placement (m/h)
- t_0 is the time up to the initialization of the concrete setting time, which the author considers its determination by Eq. (9) based on the experimental data of the CERA Report N° 1 [21].

$$t_0 = \frac{70 + 0.3\alpha - 2T}{25 + T} \quad (9)$$

where:

- t_0 is the time up to the initialization of concrete setting time (h)
- α is the concrete slump (mm)
- T is the concrete temperature (°C).

CIRIA Report 108 [10] in 1985 proposed a pressure curve according to Fig. 1b where the value of P_{max} is determined by Eq. (10) and is never greater than the hydrostatic pressure produced by a fluid with concrete density.

$$P_{max} = \left[C_1\sqrt{R} + C_2K_1\sqrt{H_1 - C_1\sqrt{R}}\right]\gamma \quad (10)$$

where:

- P_{max} is the maximum lateral pressure against formwork (kPa)
- C_1 is the coefficient that depends on the size and shape of the formwork. For walls and bases $C_1 = 1.0$
- C_2 is the coefficient that depends on the constituent materials of the concrete
- γ is the concrete specific weight (kN/m^3)
- H_1 is the vertical form height. (m)
- K_1 is the coefficient that depends on the concrete temperature given in Eq. (11)
- R is the rate of placement (m/h)

$$K_1 = \left(\frac{36}{T + 16}\right)^2 \quad (11)$$

where:

- T is the concrete temperature (°C).

The French Standard NFP 93-350 [23] considers the application of hydrostatic distribution for formwork design up to 3 m high.

Yu [24] after compiling historical data formulated an equation for predicting concrete lateral pressure using multiple linear regression techniques. The model is according to Fig. 1b, where the value of P_{max} is determined in Eq. (12) and is never greater than the hydrostatic pressure produced by a fluid with concrete density.

$$P_{max} = C_mC_f\left[31.1 + 7.8H - 0.5\,(T + 17.8) + 0.8\,(\alpha)^{1/2} - 14.8\log(t)\right] \quad (12)$$

where:

- P_{max} is the maximum lateral pressure against the formwork (kPa)
- C_m is the coefficient that depends on the constituent materials of the concrete

- C_f is the coefficient that depends on the size and shape of the formwork, for columns 1.2
- H is the concrete depth (m)
- T is the concrete temperature (°C)
- α is the concrete slump (mm)
- t is the time of concrete placement (h).

The ACI Committee 347 [9] in 2004 proposes a pressure envelope according to Fig. 1b where the maximum pressure is determined by Eq. (13). Two coefficients should be used for correcting the mix specific weight (C_W) and chemical composition and additives (C_C).

When $R < 2.1$ m/h and $H < 4.2$ m

$$P_{\max} = C_W C_C \left[7.2 + \frac{785R}{T + 17.8}\right]. \tag{13a}$$

When $R < 2.1$ m/h and $H > 4.2$ m and for all walls with $2.1\ \text{m/h} < R < 4.5\ \text{m/h}$

$$P_{\max} = C_W C_C \left[7.2 + \frac{1156}{T + 17.8} + \frac{244R}{T + 17.8}\right]. \tag{13b}$$

In both cases $P_{\max}$ should be greater than $30C_W$, but no higher than the hydrostatic pressure produced by a fluid with concrete density. where:

- $P_{\max}$ is the maximum lateral pressure against the formwork (kPa)
- R is the rate of placement (m/h)
- T is the concrete temperature (°C)
- C_W is the unit weight coefficient
- C_C is the chemistry coefficient
- H is the concrete depth (m).

ASCE 37 [25] in 2002 recommended the application of the previous ACI Committee 347 [9] model, which consisted of the same equations without the unit weight and chemistry coefficient. Barnes and Johnston [26] in 2003 recommended the implementation of coefficients C_C and C_W. They also recommended the elimination of Eq. (13a), applying in all cases the Eq. (13b) for walls, a recommendation that was not considered by the Committee.

The European standard EN 12812 [27] from 2004 states that the lateral loads from fresh concrete shall be calculated by one of the following models: CIRIA Report 108 [10] or DIN 18218 [28].

A new draft of the German standard E DIN 18218 [29] in 2008 provides a pressure envelope according to Fig. 1d where the pressure diagram extends to the minimum value between the concrete depth or the product between the rate of placement and the concrete final setting time (t_E). The value of $P_{\max}$ for normally vibrated concrete is expressed in Eq. (14). This pressure envelope is only valid for a temperature of 15 °C, a concrete specific weight of 25 kN/m^3, and a rate of placement below 7.0 m/h.

$$P_{\max} = (5R + 21)\, K_D \text{ Stiff mix} \tag{14a}$$

$$P_{\max} = (10R + 19)\, K_D \text{ Soft mix} \tag{14b}$$

$$P_{\max} = (14R + 18)\, K_D \text{ Fluid mix} \tag{14c}$$

$$P_{\max} = (17R + 17)\, K_D \text{ Liquid concrete} \tag{14d}$$

where:

- $P_{\max}$ is the maximum lateral pressure against the formwork (kPa)
- R is the rate of placement (m/h)
- K_D is a coefficient that depends on the final setting time (t_E).

Fig. 2. Ibiur dam.

This standard provides that the value of $P_{\max}$ should increase by 3% for each °C under 15 °C, and decrease by 3% for each °C over 15 °C up to a maximum reduction of 30%. Furthermore, a correction factor depending on the specific weight of the mixture is proposed.

In order to ascertain which model applies, it is necessary to perform the experimental validation, due a lack of data for pieces of concrete which have a cross section with both dimensions greater than 2 m. Moreover, obtaining more measurements during construction allows the validation and selection of the most adequate method.

Equations that can have a reasonable adequacy with respect to real lateral pressure at thicknesses less than 50 cm, may not be suitable for greater thicknesses.

Another issue is measuring the pressure by an indirect method, such as the force on the support elements of the formwork, which makes it possible to validate the integral of the pressure envelope by means of a finite element model.

Therefore, the aim of the present study is to measure real values in a dam construction, and compare them with values obtained from a finite element model performed in ABAQUS/CAE.

3. Experimental measurements

3.1. Construction site description

The measurements were conducted during the construction of a dam in Ibiur, a city located in the province of Guipúzcoa in the north of Spain. The dam is intended to supply water to several municipalities and improve the quality of the Oria River during the dry season.

The construction consists of a gravity dam with a height of 69.15 m above the foundations, a coronation length of 231.85 m requiring 176,049 m^3 of concrete for its completion. Fig. 2 shows an image of the construction.

The construction was based on building concrete blocks side by side all along the dam using climbing formworks, lifting them to complete the entire height.

3.2. Concrete blocks

Fig. 3 shows a diagram of the section of the blocks with the corresponding measurements: all of them are 15 m long, and the side slopes are 1V:0.05H and 1V:0.3H. All the experimental data were obtained on the block face with slopes of 1V:0.3H. The dimensions of the studied blocks are expressed in Table 1.

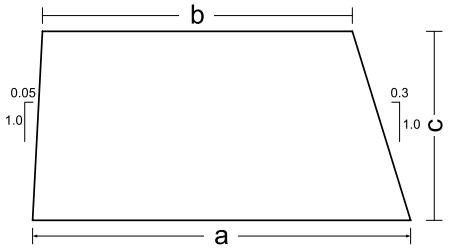

Fig. 3. Cross section of the dam's blocks.

Table 1
Block dimensions.

Block no.	Side "a" (m)	Side "b" (m)	Side "c" (m)
1	6.95	6.42	1.51
2	7.60	6.92	1.95
3	6.92	6.47	1.30
4	6.47	5.72	2.13
5	5.72	5.10	1.77
6	6.42	5.74	1.93
7	5.10	4.51	1.78
8	5.74	5.06	1.92

3.3. Concrete and filling process characteristic

The concrete mix can be considered as type IV according to ASTM C 150–07 [30], or CEM IVA/LH according to EN-1992 [31], because of the large size of the blocks, required to reduce hydration heat. With these data a coefficient $C_2 = 0.45$ must be considered in the model proposed by CIRIA Report 108 [10], a chemistry coefficient of $C_C = 1.2$ must be considered in the case of the model proposed by the ACI Committee 347 [9] and a coefficient Cm = 1.2 must be considered in the case of the model proposed by Yu [24]. For the draft of German Standard E DIN 18218 [29], a value of setting time of 5 h is considered, which represents a coefficient $K_D = 1$.

Table 2
Filling process characteristics.

Bolck no.	Rate of placement (m/h)	Temperature (°C)	Number of lifts
1	0.42	16.0	2
2	0.43	15.3	3
3	0.45	14.4	2
4	0.45	16.1	3
5	0.41	5.9	3
6	0.42	7.8	3
7	0.44	9.2	3
8	0.40	15.8	3

The concrete density is 2500 kg/m^3, having a plastic consistency with a mean slump of 30 mm.

For the correct application of the models presented above, it is necessary to know the rate of placement and the concrete's temperature. Not having any data on the mix temperature, the equation used by Lachemi and Aitcin [32] was considered to estimate the fresh concrete's temperature.

The casting process is by lifts of 65 cm height, which are mechanically vibrated. In the case of the block height not being a whole number of lifts, depending on the difference between them, another lift is made or the last one has a height greater than the others.

In Table 2, the rate of placement, temperature and number of lifts are specified for each block.

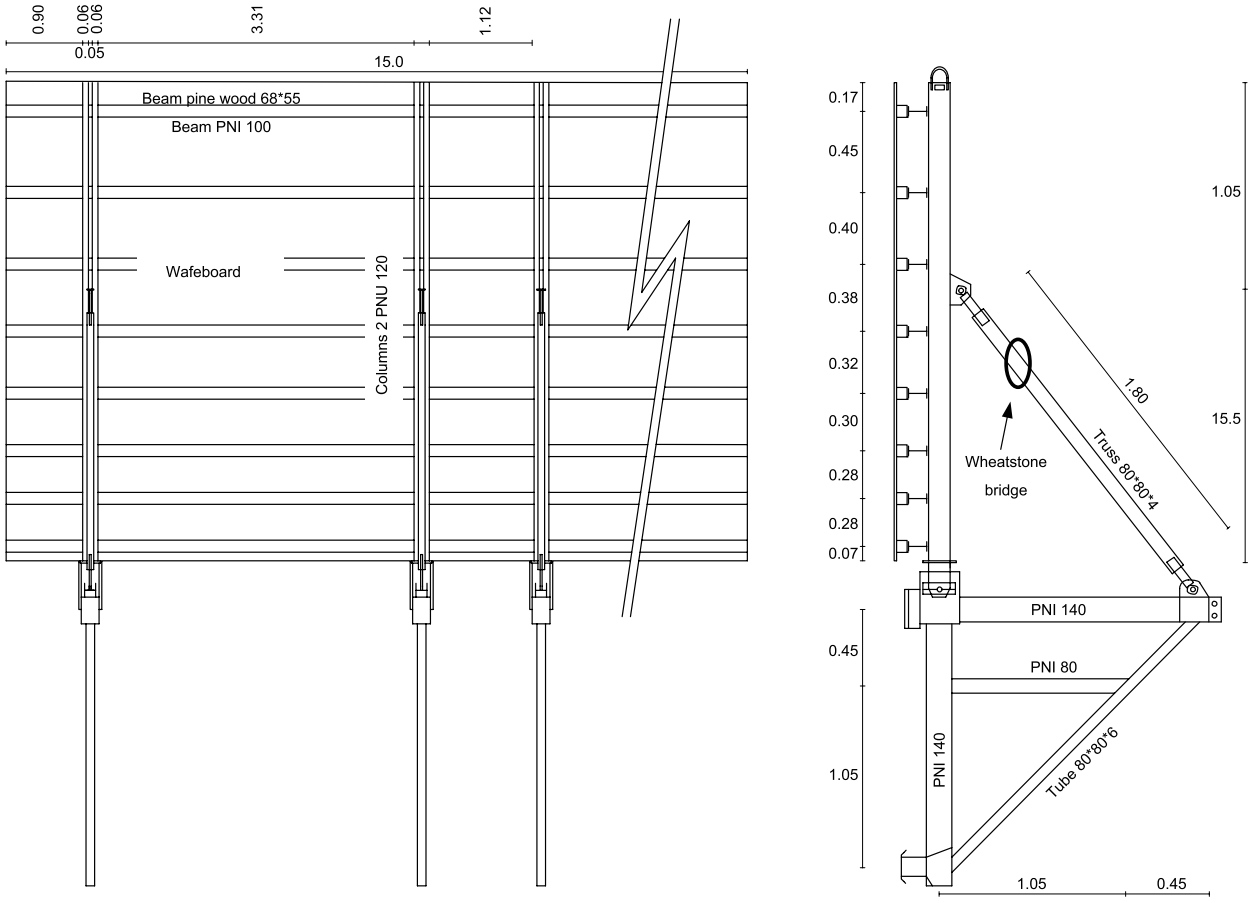

Fig. 4. Formwork plot.

Fig. 5. Instrumented trusses placed at the construction site.

3.4. Formwork

In order to measure the concrete lateral pressure, two climbing formworks, used in the construction, were instrumented. A not-to-scale plot of the formwork and support elements is shown in Fig. 4.

The formwork consists of a wafeboard panel (20 mm thick) stiffened by pine wood beams (68*55 mm) and cross section European beam I-Shape 100, which act as stiffeners. These horizontal elements are supported by 6 columns formed by 2 European beam U-Shape 120 which are supported by trusses (Tube 80*80*4) and are articulated at one extreme to the formwork support structure, as shown in Fig. 4.

The trusses (Tube 80*80*4), are articulated at both ends, one to the columns and the other to the lower structure. This structure is made of two cross sections of European beam I-Shape 140, coupled together at an angle of 90 degrees, one of them parallel with the formwork wafeboard. Other elements of the structure are as shown in Fig. 4.

3.5. Measurement system set up

The trusses (Tube 80*80*4) of the two formworks were instrumented with four strain gauges connected in a Wheatstone bridge configuration. Two active gauges were bonded on opposite arms to eliminate the influence of the bending strain, and two other gauges were placed normal to the active one to temperature compensate. All the gauges were protected against mechanical shock and humidity.

A picture of some instrumented trusses in place at the construction site is shown in Fig. 5. Before placement on the construction site, the stiffness of each steel truss was measured in a laboratory. In this calibration phase, the ratio between transmitted load and micro-strain was obtained for every truss.

Since steel shores were used, a linear relation between load and micro-strain was assumed. The mean square error between actual values and linear approximation was lower than 0.2% in all tests.

3.6. Measurements and results

The micro-strain value was almost continuously recorded, in order to obtain the maximum value for this parameter. The micro-strain value was stored every five seconds, until the casting was finished by means of a portable strain-gauge amplifier that remained on site throughout the casting process.

Table 3 shows the maximum load measure (kN) for each truss. Due to failures in connections during the casting process some measurements were not registered. The trusses are numbered from one end to the other in ascending form.

Table 3
Maximum truss load (kN).

Bolck no.	Truss no.					
	1	2	3	4	5	6
1	37.4	49.9	48.0	50.1	–	57.4
2	118.2	106.9	111.5	108.4	113.6	94.8
3	39.4	41.7	38.2	–	–	–
4	137.2	–	122.6	–	129.9	86.4
5	–	–	–	90.7	91.9	82.7
6	–	–	–	–	107.1	108.8
7	–	–	–	81.4	77.5	58.9
8	124.4	–	–	–	112.6	110.3

4. Finite element modelling

Finite element analysis was performed using the general purpose finite element code ABAQUS/CAE. Considering the envelope pressure diagram given by different authors, the theoretical load on each truss can be determined, and this value can be compared with those obtained in the field. The most important objective of the model is not only to verify the value of the maximum pressure, but to contrast the correct fitness of the entire envelope.

4.1. Model geometry

Different elements were used to ensure a good approximation to reality. The four node shell element S4R with reduced integration and hourglass control was used to model the geometry of the wood panel which can be used both for thin and thick plates. The joints between the panel and the wood beams, which act like stiffeners, are made with "ties" to guarantee that rotations and displacements at the contact faces are the same. Furthermore, this type of joint is also used to simulate the contact between the pine beams and the European beam I-Shape 100.

The columns are articulated at their lower end, and the junction "Join" at every contact with the European beam I-Shape 100 is used. This junction ensures that the displacements of both pieces at contact points are the same.

The wood beams and the steel structure, except on the trusses, are modelled with two node B31 linear beam elements.

Trusses are articulated at the ends, allowing only axial load, so element T3D2, the two node linear 3-D truss element, is used.

The points of the metal structure which are tied to the concrete are modelled with all displacement and rotations equal to zero.

Pine wood properties, as specified by Mott [33], were adopted as: Young's modulus $E = 10$ GPa, and Poisson ratio $\nu = 0.3$. For the wafeboard, $E = 4$ GPa and $\nu = 0.3$ were adopted as provided by the manufacturer. Finally, steel properties were taken as $E = 210$ GPa, and $\nu = 0.25$.

4.2. Pressure envelopes considered

The study of each block was carried out considering the lateral pressure of fresh concrete according to the pressure envelopes proposed by different authors in order to compare the degree of adequacy and safety for each model.

For comparison proposes models: Hydrostatic of a fluid with the same density than concrete, Rodin [16], Adam et al. [17], Palanca [20], CIRIA Report 108 [10], Yu [24], ACI Committee 347 [9], E DIN 18218 [29] and the recommendation proposed by Barnes and Johnston [26], not taking in care by the ACI Committee, were considered.

In case of the ACI Committee 347 [9] recommendations, due to low temperatures and rate of placement, the P_{max} obtained from Eq. (13a) gave a value lower than the proposed $30C_W$ limit in all the cases studied. Two possibilities were considered: one taking

Table 4
Load on trusses according to the different methods considered (kN).

Block no.	Trss no.	Exper. result (kN)	Hydrost. (kN)	Rodin (kN)	Adam et al. (kN)	Palanca (kN)	CIRIA (kN)	Yu (kN)	ACI Com. 347 (kN)	ACI 347 Eq. (13a) (kN)	E DIN 18218 (kN)
1	1	37.4	78.8	75.3	71.7	64.8	78.8	74.9	78.5	69.9	69.7
	2	49.9	63.9	61.1	58.2	52.6	63.9	60.9	63.7	56.7	56.6
	3	48.0	62.7	59.8	57.0	51.5	62.7	59.7	62.4	55.6	55.4
	4	50.1	62.7	59.8	57.0	51.5	62.7	59.7	62.4	55.6	55.4
	6	57.4	78.8	75.3	71.7	64.8	78.8	75.0	78.5	69.9	69.7
	Overall	242.8	347.0	331.2	315.5	285.1	347.0	330.2	345.4	307.7	306.8
2	1	118.2	146.9	127.9	132.5	126.9	141.1	132.1	139.2	116.5	123.5
	2	106.9	119.5	104.0	107.8	103.3	114.7	107.4	113.3	94.8	100.6
	3	111.5	117.0	102.0	105.7	101.2	112.4	105.3	111.0	93.0	98.5
	4	108.4	117.0	102.0	105.7	101.2	112.4	105.3	111.0	93.0	98.5
	5	113.6	119.5	104.0	107.8	103.3	114.7	107.4	113.3	94.8	100.6
	6	94.8	146.9	127.9	132.5	126.9	141.1	132.1	139.2	116.5	123.5
	Overall	653.4	767.0	667.8	692.0	662.9	736.3	689.5	726.9	608.7	645.2
3	1	39.4	51.9	51.9	50.0	45.2	51.7	51.6	51.7	49.7	49.7
	2	41.7	42.1	42.1	40.6	36.6	41.9	41.9	41.9	40.3	40.3
	3	38.2	41.2	41.2	39.7	35.8	41.0	40.9	41.0	39.5	39.5
	Overall	119.3	135.2	135.2	130.2	117.6	134.6	134.4	134.6	129.6	129.5
4	1	137.2	188.6	150.4	156.0	150.7	177.8	167.2	171.8	144.6	147.5
	3	122.6	150.3	120.2	124.6	120.3	141.8	133.5	137.1	115.5	117.8
	5	129.9	153.6	122.6	127.3	122.9	144.9	136.3	140.0	117.9	120.3
	6	86.4	188.6	150.4	156.0	150.7	177.8	167.2	171.8	144.6	147.5
	Overall	476.1	681.1	543.6	564.0	544.7	642.4	604.2	620.5	522.5	533.0
5	4	90.7	91.3	81.0	79.0	80.3	91.3	88.9	88.3	83.2	85.3
	5	91.9	93.3	82.6	80.6	81.9	93.3	90.7	90.1	84.9	87.1
	6	82.7	114.8	101.7	99.2	100.8	114.8	111.7	110.9	104.5	107.2
	Overall	265.3	299.4	265.3	258.9	262.9	299.4	291.3	289.2	272.5	279.7
6	5	107.1	116.4	98.9	96.0	98.3	116.4	110.1	109.4	100.5	103.5
	6	108.8	143.1	121.6	118.0	120.8	143.1	135.3	134.5	123.6	127.2
	Overall	216.0	259.5	220.5	214.0	219.1	259.5	245.4	244.0	224.1	230.6
7	4	81.4	94.3	93.0	89.7	80.0	94.3	90.9	91.7	84.7	86.0
	5	77.5	96.3	95.0	91.5	81.6	96.3	92.8	93.6	86.4	87.8
	6	58.9	118.5	116.9	112.6	100.4	118.5	114.2	115.1	106.3	108.0
	Overall	217.9	309.0	304.9	293.9	261.9	309.0	297.9	300.4	277.4	281.7
8	1	124.4	142.4	120.2	130.0	122.9	137.1	127.5	134.5	111.7	114.4
	5	112.6	115.8	97.7	105.8	100.0	111.5	103.7	109.4	90.9	93.1
	6	110.3	142.4	120.2	130.0	122.9	137.1	127.5	134.5	111.7	114.4
	Overall	347.4	400.5	338.0	365.7	345.8	385.6	358.7	378.5	314.3	322.0

the exact formulation of the Committee and another which did not consider the lower limit of the maximum pressure and took the value of P_{max} directly from Eq. (13a).

Eqs. (4a) and (4b) were used for modelling Adam et al. [17] depending on the temperature and for E DIN 18218 [29], Eq. (14a) was used for determining the pressure envelope.

The distribution proposed by Gardner [18] was not studied because the same author in [5] does not recommend its application to walls with thicknesses greater than 1 m. Johnston et al. [12] verified the poor adaptation of this theory to a thickness of 1.2 m.

4.3. Model results

Table 4 shows the results of truss forces (kN) obtained from the different methods considered, compared with experimental results. Those values are ordered by block as well as truss number.

The results obtained from the recommendations proposed by Barnes and Johnston [26] are not present in Table 4 because in all the cases the blocks were not high enough to reach the maximum pressure, so the distribution is the same as the hydrostatic one.

The main causes of this coincidence are the low temperature and rate of placement. The second term of the Eq. (13b) is approximately 4 times greater than the other two so P_{max} appears to be around 3 m.

5. Comparison of the results

To compare the results obtained by the different methods with the experimental data, Fig. 6 shows the experimental load on each truss of the different blocks vs. the load obtained applying the considered theoretical model; different marks were utilised for different blocks. The line which represents the experimental load equal to the theoretical values is also drawn for analysing the safety of the different methods.

5.1. Trusses statistical discussion

It is difficult to quantify the relative adequacy of the methods considered to describe the experimental results from Fig. 6. In order to make a comparison, the following statistical parameters will be used: mean of the ratio experimental load/theoretical load (Eq. (15)), standard deviation of the ratio experimental load/theoretical load (Eq. (16)), Pearson correlation coefficient squared (Eq. (17)), standard error (Eq. (18)) and an adaptation of the reliability index proposed in UNE EN 1990 [34]. Gardner [5] feels that a linear regression is not appropriate because the experimental and theoretical values are neither dependent nor independent variables.

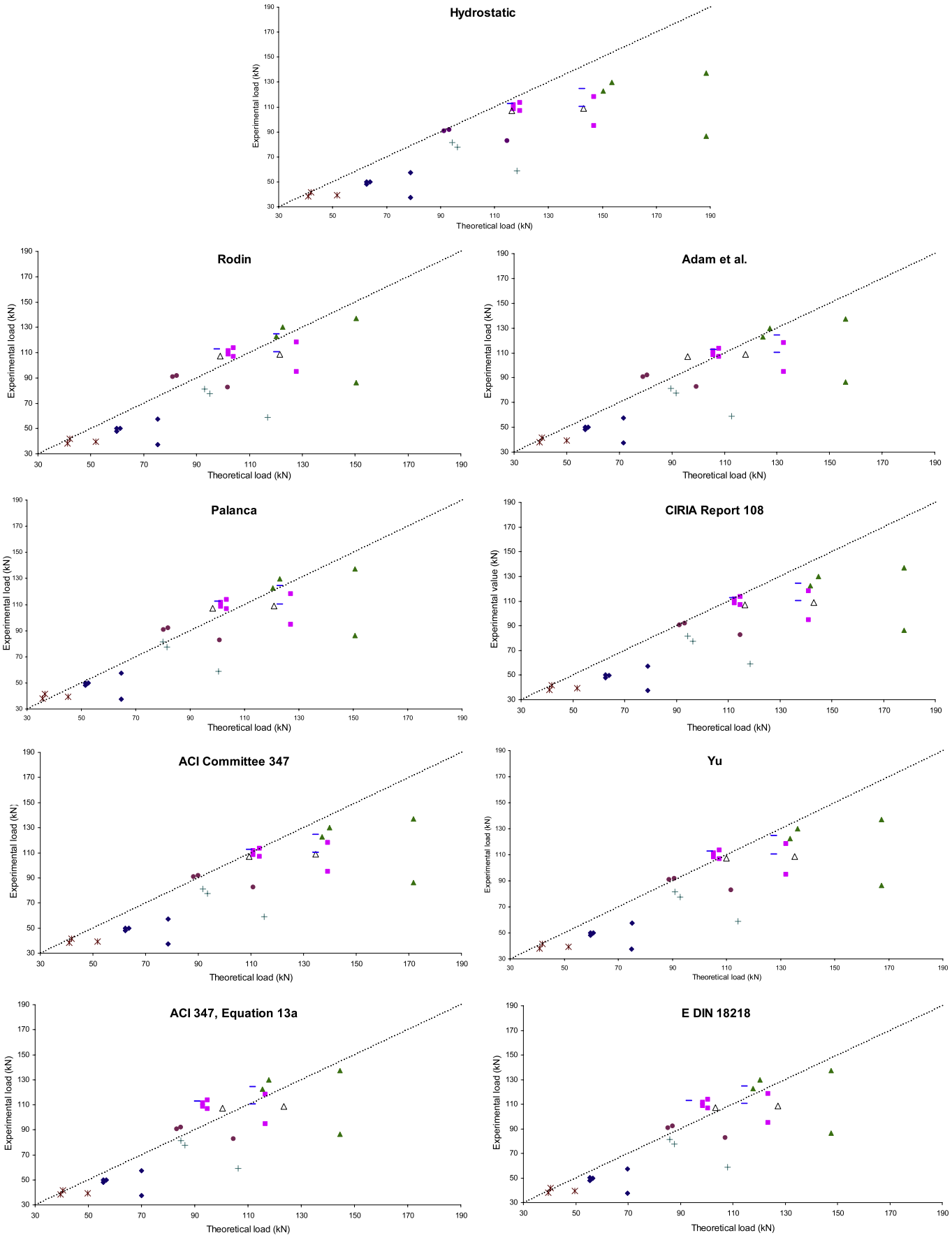

Fig. 6. Comparison of the results.

Table 5
Truss statistical comparison of the results.

Theory	Mean of ratio E_i/T_i	Standard deviation of ratio E_i/T_i	Pearson correl. coefficient squared	Standard error (kN)	Reliability index
Hydrostatic	0.807	0.148	0.692	31.55	1.02
Rodin	0.904	0.179	0.642	21.11	0.48
Adam et al.	0.902	0.168	0.685	21.15	0.54
Palanca	0.952	0.163	0.725	18.06	0.32
CIRIA	0.825	0.152	0.686	28.45	0.96
Yu	0.866	0.160	0.674	24.07	0.72
ACI Committee 347	0.842	0.155	0.686	26.11	0.87
ACI 347 (Eq. (13a))	0.955	0.186	0.648	18.99	0.22
E DIN 18218	0.931	0.173	0.672	19.24	0.36

– Mean of the ratio experimental load/theoretical load:

$$\mu_{\frac{E}{T}} = \frac{\sum_{i=1}^{n} \frac{E_i}{T_i}}{n}. \tag{15}$$

– Standard deviation of the ratio experimental load/theoretical load:

$$\sigma_{\frac{E}{T}} \sqrt{\frac{\sum_{i=1}^{n} \left(\frac{E_i}{T_i} - \mu_{\frac{E}{T}}\right)^2}{n-1}}. \tag{16}$$

– Pearson correlation coefficient squared:

$$PCC = \left(\frac{n \sum_{i=1}^{n} E_i T_i - \left(\sum_{i=1}^{n} E_i\right)\left(\sum_{i=1}^{n} T_i\right)}{\sqrt{\left[n \sum_{i=1}^{n} E_i^2 - \left(\sum_{i=1}^{n} E_i\right)^2\right]\left[n \sum_{i=1}^{n} T_i^2 - \left(\sum_{i=1}^{n} T_i\right)^2\right]}} \right)^2. \tag{17}$$

– Standard error (kg):

$$SE = \sqrt{\frac{\sum_{i=1}^{n} (E_i - T_i)^2}{n}} \tag{18}$$

where:
- E_i is the experimental value from the observation "i".
- T_i is the theoretical value calculates from the observation "i".
- n is the number of observations.

The standard UNE EN-1990 [34] states that the probability of failure can be expressed through a performance function g. A structure is considered to be safe if $g > 0$ and to fail if $g < 0$. If R is the resistance and F is the effect, the function g is defined in Eq. (19).

$$g = R - F. \tag{19}$$

If g is normally distributed, the reliability index is determined by Eq. (20).

$$\beta = \frac{\mu_g}{\sigma_g} \tag{20}$$

where:

- β is the reliability index
- μ_g is the mean of function g
- σ_g is the standard deviation of function g

For other distributions of g, β is only a conventional measurement of the reliability index. An adaptation of the method has been considering in the study case considering the finite element model results as the resistance R and the experimental results as the effect F. This assumption brings small values of the reliability index to the structure because the safety factor is not considered.

The results for the different models are expressed in Table 5. These coefficients are only indicators of the alignment in the adjustment and are used only to compare the different models.

Based on the mean of the ratio E_i/T_i, Eq. (13a) proposed by the ACI Committee 347 [9] is the model that best fits the results. But analysing the standard deviation of the ratio E_i/T_i, this theory presents the largest value, and have a lower value for the reliability index. This exemplifies the difficulty in quantifying one by one the relative adequacy of theoretical models, but it is possible to analyse the results of the overall statistics.

Based on the first two statistics, the three theories that best fit the experimental data are: E DIN 18218 [29], Palanca [20] and Eq. (13a) proposed by ACI Committee 347 [9]. This idea can be reaffirmed by observing the standard error. Considering the reliability index this theory presents the lowest value signifying a higher risk in the design, but the structure present a safety factor which is not considered in this analysis.

If the comparison is based on the Pearson correlation coefficient squared, Palanca [20] theory has a slight advantage over the other methods studied.

5.2. Block statistical discussion

Whit the objective of clarifying the comparison it is important to study the different blocks as a unit, Puente et al. [35] state that formwork characteristics can affect the force of each truss producing a significant variation, while the entire load is in a very good agreement with the one obtained from theoretical models.

Comparing the sum of the experimental data with the sum of the force in each truss, facilitates making a comparison between the total real and theoretical effects that concrete produces.

In Table 4, are presented for each block the overview of the different theories, and the same statistical parameters utilised in the truss force comparison are presented for the overall values in Table 6, maintaining a high relationship with the results presented for trusses in terms of the different model approaches.

Based on the results presented in Table 6, the theories which best reflect the experimental values were E DIN 18218 [29], Palanca [20] and Eq. (13a) proposed by ACI Committee 347 [9], which is consistent with the results obtained for a single truss analysis. The main difference between the models is in the maximum ratio between the sum of experimental and theoretical forces being 1.08, 1.01 and 1.10 respectively, which indicates that Palanca [20] has a lower risk.

The ACI Committee 347 [9], CIRIA Report 108 [10] and Yu [24] models are more conservative because they do not establish for any block a value higher than the overall experimental results, this reflects that the hydrostatic distribution is not adequate for design since it because is more conservative than these models.

Yu [24] is the most adequate theory in comparison with ACI Committee 347 [9] and CIRIA Report 108 [10] based on the data presented in Table 6.

Table 6
Block statistical comparison of the results.

Theory	Mean	Standard deviation	Pearson correl. coefficient squared	Standard error (kN)
Hydrostatic	0.803	0.086	0.953	100.12
Rodin	0.899	0.121	0.946	50.61
Adam et al.	0.900	0.105	0.963	50.96
Palanca	0.945	0.078	0.978	32.65
CIRIA	0.817	0.088	0.955	85.46
Yu	0.856	0.093	0.952	64.84
ACI Committee 347	0.838	0.090	0.958	75.94
ACI 347 (Eq. (13a))	0.940	0.116	0.948	40.66
E DIN 18218	0.919	0.103	0.961	39.73

Table 7
Corrective standard error as a function of coefficient K.

Theory	Values of "K" for less SE_K	Value of "K" $SE_K = SE_{(Hydrostatic)}$
Palanca	$1 \leq K < 13$	$K = 25$
Yu	$13 \leq K < 21$	$K = 72$
ACI Committee 347	$21 \leq K < 203$	$K = 464$
CIRIA Report 108	$203 \leq K < 4090$	$K = 4090$
Hydrostatic	$K > 4090$	–
Rodin	–	$K = 21$
Adam et al.	–	$K = 32$
ACI 347 (Eq. (13a))	–	$K = 9$
E DIN 18218	–	$K = 17$

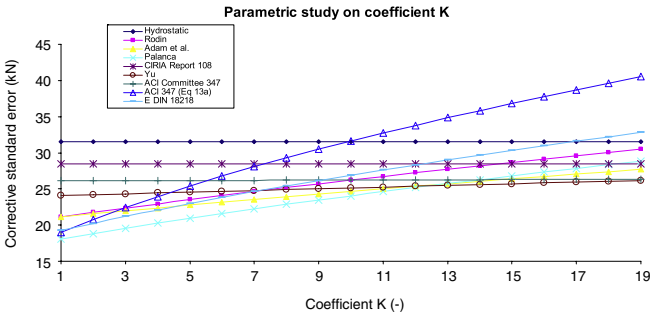

Fig. 7. Plot corrective standard error vs. coefficient K.

5.3. Security in the problem

The objective of a theoretical model that has to be used in the design process of the formwork and the support elements is not just looking for a good adjustment to the real lateral pressure realised by fresh concrete, but also to maintain a minimum safety factor. This idea has to be kept in mind when selecting the theoretical model.

Any point in Fig. 6 that has an experimental load value greater than the theoretical data has to be considered "unsafe", because the real force is greater than the one predicted; it is an underestimation of the real load which can cause failure.

To take into account the influence of these "unsafe" points in the calculation of formwork and their support elements, a "K" coefficient, greater or equal to one has been used to determine a corrective standard error (SE_K). The definition of the corrective standard error is given in Eq. (21).

$$SE_K = \sqrt{\frac{\sum_{E_i \leq T_i} (E_i - T_i)^2 + K \sum_{E_i > T_i} (E_i - T_i)^2}{n}}. \quad (21)$$

This coefficient allows us to increase the difference when determining the corrective standard error for "unsafe" points. This way it is possible to determine the method which presents the lowest value in the corrective standard error in function of the coefficient K.

The assumption of hydrostatic pressure as equal to concrete pressure does not present any "unsafe" points. Therefore, the coefficient K does not influence this distribution. This states that from a certain value of the coefficient the hydrostatic pressure is going to have the lowest corrective standard error.

This study is only realised for the truss forces, because the experimental data has a major difference with the predictive values compared with the case of the block analysis, and in this study distribution like ACI Committee 347 [9], CIRIA Report 108 [10] and Yu [24] do not present changes between the standard error and the corrective standard error.

Table 7 shows which method presents the smallest value of corrective standard error in the function of the coefficient K, and which is the value of the coefficient that makes the corrective standard error of the different theoretical methods the same as that obtained for hydrostatic distribution. Fig. 7 plotted the corrective standard error vs. the value of the coefficient K for the different methods considered.

Table 7 and Fig. 7 show that Palanca [20] is the theory that best fits the theoretical problem while presenting several "unsafe" points. As the parameter K increases it becomes less appropriate. Yu [24] is the best method for a small parameter interval the next best is ACI Committee 347 [9], then CIRIA Report 108 [10] and finally the hydrostatic distribution.

Fig. 7 shows that the influence of the "unsafe" points on the theory ACI 347 (Eq. (13a)), is quite significant for establishing the correct formulation of the lower pressure limit $30C_W$. The corrective standard error of this theory grows with the coefficient K to a significantly higher degree than in other theories.

Table 7 shows the value of parameter K, than makes the corrective standard error equal to the one in the hydrostatic distribution. The value of ACI 347 (Eq. (13a)) is the lowest, as mentioned above. This value for the theories: Rodin [16], Adam et al. [17], DIN 18218 [18] and Palanca [20], is within a very close range, suggesting that the prediction of the lateral pressure has more or less the same degree of safety in all these theories. Simultaneously, Palanca [20] is the method which presents the lowest value of SE_K in the majority of this range and which is most adequate with respect to the experimental values in the statistic parameters considered above.

ACI Committee 347 [9], CIRIA Report 108 [10] and Yu [24] are slightly more conservative theories since they have a smaller amount of "unsafe" points, being Yu [24] the more adequate and risk model according to data presented in Tables 5 and 6.

Engineers should decide whether to use a more or less conservative model depending on the construction process. Every structure has a minimum value of the coefficient K for which it could be dimensioned in a safe way. This minimum value depends on the safety factor, monitoring of the work, degree of planning and knowledge of the subject.

5.4. Safety factor

The most proper theory to be use, in each case, is determined by the minimum value of the parameter K for which the structure

is designed in a safe way. This value depends as explained above on the safety factor, the monitoring of the work, the degree of planning and knowledge of the subject.

The ACI Committee 347 [9] proposes a minimum safety factor for formwork structures, which have to support their own weight and the lateral pressure of fresh concrete in 2.0.

Paez [36] believes that all structures have a difference between the theoretical value of the security coefficient and the real one. This idea is reinforced by Randall [37], stating that the real safety factor of a structure may be greater than the projected one. That succeed when a construction is done with a high degree of vigilance and planning, taking into account the considerations set by Sommers [38]:

- Degree of coincidences between formwork plot and the real disposition in the field.
- Determine a rate of placement in the design process, and not exceeding it when casting.
- Carefully vibrate the concrete to avoid vibration longer than the depth of each lift.
- Taking into account the concrete temperature when casting
- Verify the formwork supporting elements.
- Check the formwork construction with the plot before casting.
- Intense control during the casting process.

If the construction complies with all these considerations, according to Randall [37] as mentioned above, the real safety factor of the structure is greater than the projected one and this difference can be use to absorb the different between the real load and the predicted one for "unsafe" points. These considerations allow the use of a less conservative theory which is closer to the experimental data.

In the model proposed by Palanca [20], the maximum difference of an "unsafe" point is 13%, a similar value to that is proposed by Paez [39], which sustains that the projected safety factor of a structure increase, if the construction meets that which is specified above. This way the theoretical safety factor is still present to ensure the security of the construction project.

If the planning, design and work control are not adequate, it is recommended to use a more conservative theory such as the one proposed by Yu [24] or ACI Committee 347 [9].

6. Conclusion

After obtaining the pressure value of vibrated concrete from a force determined experimentally, it was possible to evaluate the accuracy of different theoretical methods, making it possible to draw the following conclusions:

1. The hypothesis that the pressure exerted by fresh concrete is equal to the hydrostatic pressure of a liquid with the same density of the mix is conservative compared to the results obtained by other models studied
2. The recommendation made by Barnes and Johnston [26] which was not considered by ACI Committee 347 [9] coincides with the hydrostatic distribution because the low rate of placement, low temperature and dimensions of the concrete blocks do not reach the value of P_{max}. This underscores that the Committee was right not to consider that recommendation.
3. The equation proposed by CIRIA Report 108 [10] can also be considered conservative because in several blocks the distribution was the same as a hydrostatic one.
4. The limitation on the maximum pressure to a minimum value of $30C_W$, by the ACI Committee 347 [9], is appropriate because without considering this limit the presence of "unsafe" points becomes excessive.
5. Different theories for the process of formwork design, are proposed depending on the degree of planning and work supervision. If the construction project meets the criteria established by Sommers [38], the theory proposed by Palanca [20] is recommended; otherwise a more conservative model, such as that proposed by Yu [24] or ACI Committee 347 [9] may be more appropriate.
6. The model proposed by Yu [24] is more adequate than the ACI Committee 347 [9] model, but the latter has the advantage of being easier to apply and requiring less knowledge about fewer parameters for predicting the lateral pressure.
7. Palanca's [20] model has the disadvantage of being a more complex distribution than the others because it takes into account an area of soil pressure. Nevertheless, the author considers the slump test to be the basic parameter for determining the distribution. This underscores the necessity of including this value in the design process.

Acknowledgements

This research was sponsored by Ulma Construcción, and the authors also wish to acknowledge their collaboration in the collection of experimental data. The opinions expressed in this work are those of the writers and do not necessarily reflect the points of view of the company.

References

[1] Peurifoy RL, Oberlender GD. Formwork for concrete structures. 3th edition Construction Series, McGraw-Hill; 1995.
[2] Hurd MK. Formwork for concrete. 7th edition Farmington Hills: American Concrete Institute; 2005.
[3] Kopczynski C. Formwork Efficiencies. Concrete International 2008;30(06): 41–3.
[4] Gardner NJ, Quereshi AR. Internal vibration and the lateral pressure exerted by fresh concrete. Canad J Civil Eng 1979;6:592–600.
[5] Gardner NJ. Pressure of concrete on formwork — A review. ACI J 1985;82(5): 744–53.
[6] Gardner NJ, Poon SM. Time and temperature effects on tensile bond, and compressive strengths. ACI J 1976;73(7):405–9.
[7] Schjödt R. Calculation of pressure of concrete on forms. Proc ASCE 1955;81: 1–16.
[8] Levitsky M. Analytical determination of pressure on formwork. Proc ASCE 1973;99:551–64.
[9] ACI Committee 347. Guide to Formwork for Concrete. ACI Standard; 2004. p. 1–32.
[10] CIRIA Report 108 (Construction Industry Research and Information Association). Concrete pressure on formwork. 1985. 31 pp.
[11] Ritchie AGB. The pressure developed by concrete on formwork (Part I). Civil Eng Public Works Rev 1962;57:885–8.
[12] Johnston DW, Kahn KP, Phillips JB. Formwork pressures in tall and thick concrete walls. J Constr Eng Manage, ASCE 1989;115:444–61.
[13] Dunston SD, Johnston DW, McCain PP. Formwork pressures in tall walls with extended set concrete. Concr Int 1994;16(11):26–34.
[14] Arslan M, Şimşek O, Subaşi S. Effects of formwork surface materials on concrete lateral pressure. Constr Build Mater 2005;19(4):319–25.
[15] Hurd MK. Lateral pressures for formwork design. Concr Int 2007;29(06):31–3.
[16] Rodin S. Pressure of concrete on formwork. Inst Civil Eng 1953;1:709–46.
[17] Adam M, Bennasr M, Santos Delgado H. Poussée du béton frais sur les coffrages. Annales, Institut Technique du Bâtiment et des Travaux Publics (Paris) 1965; 78:403–23.
[18] Gardner NJ. The effect of superplasticizer and flyash on formwork pressures. Forming Economical Concrete Buildings, Portland Cement Association; 1982. p. 1–12.
[19] CSA S269.3. Concrete formwork. A National Standard of Canada. Rexdale, Ontario. 1992 Reaffirmed 2008. 40 pp.
[20] Palanca MJ. Presión del hormigón fresco. Monografía 371 del Instituto Eduardo Torroja de Ciencias de la Construcción. 1982. 55 pp.
[21] CERA Report No 1 (Civil Engineering Research Association). The pressure of concrete on formwork Report No 1965. (Now Reached Construction Industry Research and Information Association (CIRIA)).
[22] Gardner NJ. Pressure of concrete against formwork. ACI J 1980;77(4):279–86.
[23] NFP 93-350. French Standard. Banches industrialisées pour ouvrages en béton. 1995.

[24] Yu DN. Modeling and Predicting concrete lateral pressure on formwork. Ph.D. thesis. Institute of Construction, Dept. of Civil Engineering. North Carolina State University; 2000. 204 pp.
[25] ASCE 37. Design loads on structures during construction. American Society of Civil Engineers; 2002. 48 pp.
[26] Barnes JM, Johnston DW. Fresh Concrete Lateral pressure on formwork. Construction research. Congress wind of change: Integration and innovation; 2003. 8 pp.
[27] EN 12812. Performance requirements and general design. European Standard; 2004.
[28] DIN–18218. Frishbeton auf lotrechte pressure of concrete on vertical formwork. Deutsches institut füf normung. 1980. 4 pp.
[29] E DIN–18218. Frishbetondruck auf lotrechte Schalungen. Deutsches institut füf normung. 2008. 16 pp.
[30] ASTM C 150–07. Standard specification for portland cement. 2007. 8 pp.
[31] EN 1992. Design of concrete structures. European Standard. 2004.
[32] Lechemi M, Aitcin PC. Influence of ambient and fresh concrete temperature on the maximum temperature and thermal gradient in a high-performance concrete structure. ACI Mater J 1997;94(2):102–10.
[33] Mott RL. Applied strength of materials. 4th edition Prentice Hall; 2002.
[34] UNE EN 1990. Base de cálculo de estructuras. Eurocódigos. 2002.
[35] Puente I, Azkune M, Insausti A. Shore-slab interaction in multistory reinforced concrete buildings during construction: An experimental approach. Eng Struct 2006;29(5):731–41.
[36] Paez Balaca A. El coeficiente de seguridad. Revista de Obras Públicas; 1951. p. 253–60.
[37] Randall Jr FA. Historical Notes on Structural Safety. ACI J Proc 1973;70(10): 669–81.
[38] Sommers PH. Better construction practices for greater formwork safety. Concr Int 1982;4(05):31–9.
[39] Paez Balaca A. El coeficiente de seguridad. Revista de Obras Públicas; 1951. p. 315–23.